# Prediction of human intestinal first-pass metabolism of 25 CYP3A substrates from *in vitro* clearance and permeability data

Michael Gertz, Anthony Harrison, J. Brian Houston and Aleksandra Galetin

School of Pharmacy and Pharmaceutical Sciences, University of Manchester, Manchester, United Kingdom (MG, JBH and AG)

Pfizer Global Research & Development, Pharmacokinetics, Dynamics and Metabolism Department, Sandwich, United Kingdom (AH)

1

**Running title**: Prediction of human intestinal first-pass metabolism

**Corresponding author**:     Dr A. Galetin

School of Pharmacy and Pharmaceutical Sciences,

University of Manchester, Stopford Building

Oxford Road,

Manchester, M13 9PT, UK

Tel: (+) 44 161 275 6886

Fax: (+) 44 161 275 8349

Email: Aleksandra.Galetin@manchester.ac.uk

**Tables**:     5

**Figures**:     5

Abstract: 248

Introduction 715

Discussion: 1,680

Reference: 48

**Abbreviations**: $F_G$, intestinal availability; $P_{app}$, apparent permeability; $P_{eff}$, effective permeability; HLM, human liver microsomes; HIM, human intestinal microsomes; $CL_h$, hepatic blood clearance; $CL_{int,h}$, hepatic intrinsic clearance; $CL_{int,g}$, intestinal intrinsic clearance; $Q_{Gut}$, hybrid parameter of blood flow and drug permeability; $Q_h$, hepatic blood flow; $R_b$, blood to plasma distribution ratio; PSA, polar surface area ; HBD, hydrogen bond donors.

## Abstract

Intestinal first-pass metabolism may contribute to low oral drug bioavailability and drug-drug interactions, particularly in the case of CYP3A substrates. The current analysis predicted intestinal availability ($F_G$) from i*n vitro* metabolic clearance and permeability data of 25 drugs using the $Q_{Gut}$ model. The drug selection included a wide range of physicochemical properties and *in vivo* $F_G$ values (0.07-0.93). *In vitro* clearance data ($CLu_{int}$) were determined in human intestinal (HIM) and three liver (HLM) microsomal pools (n=105 donors) using the substrate depletion method. Apparent drug permeability ($P_{app}$) was determined in Caco-2 and MDCK-MDR1 cells under isotonic conditions (pH=7.4). Additionally, effective permeability ($P_{eff}$) data, estimated from regression analyses to $P_{app}$ or physicochemical properties were utilized in the $F_G$ predictions. Determined $CLu_{int}$ values ranged from 0.022 to 76.7μL/min/pmol CYP3A (zolpidem and nisoldipine, respectively). Differences in $CLu_{int}$ values obtained in HIM and HLM were not significant after normalization for tissue specific CYP3A abundance, supporting their inter-changeable usability. The $F_G$ predictions were most successful when $P_{app}$ data from Caco-2/MDCK-MDR1 cells were directly used; in contrast, the use of physicochemical parameters resulted in significant $F_G$ under-predictions. Good agreement between predicted and *in vivo* $F_G$ was noted for drugs with low to medium intestinal extraction (e.g., midazolam predicted $F_G$ value 0.54, *in vivo* value 0.51). In contrast, low prediction accuracy was observed for drugs with *in vivo* $F_G<0.5$, resulting in considerable under-prediction in some instances, as in the case of saquinavir (predicted $F_G$ is 6% of the observed value). Implications of the findings are discussed.

## Introduction

CYP3A enzymes represent the principle drug metabolizing system in the small intestine accounting for approximately 80% of total P450 content (Lin et al., 1999; Paine et al., 2006). Although the total amount of CYP3A expressed in the human small intestine represents approximately 1% of the hepatic estimate (Paine et al., 1997) considerable drug extraction occurs during absorption of orally administered drugs (Hall et al., 1999; Galetin et al., 2008; Gertz et al., 2008a). This is due to the relatively high enterocytic drug concentration and the considerably lower blood flow to the intestine in comparison to the liver that allows prolonged exposure to the intestinal metabolizing enzymes. The contribution of intestinal first-pass metabolism has been shown indirectly for a number of CYP3A drugs administered both intravenously and orally in the absence and presence of inhibitors/inducers (Galetin et al., 2010). Such studies have allowed delineation of the relative roles of the liver and intestine and are particularly abundant for midazolam, and to lesser extent for cyclosporine, tacrolimus, alfentanil and nifedipine.

The ability to predict the intestinal first-pass metabolism of drugs is of considerable importance for the assessment of oral clearance and drug-drug interaction (DDI) potential of CYP3A substrates. In both cases prediction models are very sensitive to the accuracy of the $F_G$ estimate and the contribution of intestinal first-pass metabolism cannot be ignored. Two indirect methods have been proposed to estimate $F_G$ *in vivo*, namely use of plasma concentration-time profiles after either oral and i.v. administration or in the presence and absence of the grapefruit juice. Both methods have several assumptions that may lead to potential bias in the $F_G$ estimates (Galetin et al., 2008; Gertz et al., 2008a).

In addition, *in silico* approaches have been proposed to estimate $F_G$. These are based on the incorporation of drug permeability and metabolism data, enterocytic blood flow together with zonal and cellular heterogeneous distribution of metabolic enzyme and efflux/uptake transporters along the length of the intestine (Ito et al., 1999; Tam et al., 2003; Badhan et al., 2009; Jamei et al., 2009). In contrast to complex physiologically-based models,

a "minimal" $Q_{Gut}$ model has been proposed. This model allows prediction of $F_G$ utilizing determined *in vitro* drug clearance and permeability (Chalasani et al., 2002; Rostami-Hodjegan and Tucker, 2002; Yang et al., 2007) and accounts for either permeability or perfusion as the rate limiting process in the small intestine (see Material and Methods, Eq. 2). However, the suitability of this model has yet to be demonstrated for a broad number of drugs. Yang et al. (2007) investigated the $F_G$ prediction success of the $Q_{Gut}$ model using *in vitro* clearance and permeability data collated from a variety of sources; while promising, this study did not allow a comprehensive assessment of the $Q_{Gut}$ model. Also, a systematic assessment of the predictive utility of different *in vitro* systems to generate either clearance or permeability data for input parameters in this model is currently lacking.

This study aims to investigate several aspects of the use of the $Q_{Gut}$ model to predict $F_G$ from *in vitro* data. First, a comparison was made between human intestinal and liver microsomes in their capacity to assess the metabolic drug clearance of a large number of structurally diverse drugs using a range of commercially available microsomal pools. The current analysis involves 25 drugs with differing physicochemical, metabolic and permeability properties (Table 1 and Table 3). These drugs also show differing extents of intestinal first-pass metabolism *in vivo* with $F_G$ values ranging from 0.07-0.94 for lovastatin and alprazolam, respectively. The suitability of these *in vitro* clearance data to predict both i.v. and oral clearance (incorporating the available *in vivo* $F_G$) was explored. Secondly, the use of permeability data ($P_{app}$ (A-B)) generated under standardized conditions in both MDCK-MDR1 and Caco-2 cell lines was investigated, together with effective permeability ($P_{eff}$), as permeability input parameters in the $Q_{Gut}$ model. The latter parameter was estimated either from regression analysis of the Caco-2 and MDCK-MDR1 data or from physicochemical parameters. Finally, the value of using midazolam as a calibrator within the $Q_{Gut}$ model was investigated given the abundance of information on this drug both *in vivo* and *in vitro*. On the basis of these analyses, recommendations on the suitability of the various *in vitro* input parameters in the $Q_{Gut}$ model and associated prediction accuracy are discussed.

## Materials and Methods

**Prediction of intestinal availability.** The $CLu_{int}$ values were scaled by the total amount of intestinal CYP3A to an intestinal intrinsic clearance, $CL_{int,g}$ (Eq. 1). The total CYP3A content used in the current analysis was 70.5nmol (Paine et al., 1997). The $F_G$ values were predicted using the $Q_{Gut}$ model (Chalasani et al., 2002; Rostami-Hodjegan and Tucker, 2004) as defined in Eq. 2. $Q_{Gut}$ represents a hybrid parameter of enterocytic blood flow and drug permeability as defined by Eq. 3 (Yang et al., 2007). $F_G$ predictions from $Q_{Gut}$ model were compared to *in vivo* $F_G$ estimates obtained either from i.v./oral or grapefruit interaction data (Galetin et al., 2008; Gertz et al., 2008a) and summarized in Table 5. In the case of indinavir, $F_G$ value was estimated from i.v./oral data reported by Yeh et al. 1999.

$$CL_{int,g} = CLu_{int} \cdot Content_{CYP3A} \qquad \text{Eq. 1}$$

$$F_G = \frac{Q_{Gut}}{Q_{Gut} + fu_{Gut} \cdot CL_{int,g}} \qquad \text{Eq. 2}$$

$$Q_{Gut} = \frac{CL_{perm} \cdot Q_{ent}}{Q_{ent} + CL_{perm}} \qquad \text{Eq. 3}$$

where $F_G$ represents intestinal availability, $Q_{Gut}$, hybrid parameter of blood flow and drug permeability (L/h), $Q_{ent}$, mucosal blood flow (L/h), $CL_{int,g}$, unbound intrinsic gut clearance (L/h), $fu_{Gut}$, fraction unbound in the enterocytes, $CL_{perm}$, permeability clearance (L/h), product of intestinal surface area and either apparent (nm/s) or effective permeability (µm/s); $CL_{int,g}$, intestinal intrinsic clearance (L/h).

The fraction unbound in the enterocytes was assumed to be 1 (Yang et al., 2007) and an average enterocytic blood flow ($Q_{ent}$) of 18L/h was used for the predictions (Granger et al., 1980). Use of either fu in plasma or blood as an alternative to $fu_{Gut}=1$ resulted in complete loss of prediction success and $F_G$ values approaching 1 for all drugs investigated. In the case where effective permeability was used to predict $F_G$, an intestinal surface area of $0.66m^2$ (intestine treated as a tube as $P_{eff}$ accounts for the surface area magnifications of the fold of Kerkering, the villi and microvilli) was used to estimate permeability clearance (Yang et al., 2007). If apparent permeability was used to estimate permeability clearance an intestinal surface area of $200m^2$ was used.

**Midazolam as $Q_{Gut}$ calibrator.** In order to define a maximal value for $Q_{Gut}$ that approaches mucosal blood flow, the use of midazolam as a calibrator was investigated. Midazolam was selected as this drug is characterized by high apparent permeability. The $Q_{Gut}$ value of midazolam was estimated from the mean *in vitro* $CLu_{int}$ data determined in this study and the mean $F_G$ value *in vivo* determined from 16 i.v./oral studies (Galetin et al., 2008) by rearranging Eq. 2. The assumptions were that enterocytic binding is negligible ($fu_{Gut}=1$) and that midazolam *in vitro* clearance is representative of its *in vivo* clearance. The $F_G$ *in vivo* for midazolam ranged from 0.49 to 0.70 (Galetin et al., 2008) and the $CL_{int,g}$ ranged from 7.30 to 28.7L/h (Table 1). The coefficient of variation on the mean $Q_{Gut}$ value of midazolam was assessed by taking into account the variability of *in vivo* data ($F_G$) or both *in vivo* and *in vitro* clearance data.

**Determination of *in vitro* clearance.** The *in vitro* clearance data were determined by depletion in three liver and one human intestinal microsomal pools in 0.1M phosphate buffer (pH 7.4) containing 10mM $MgCl_2$, 7.5mM isocitric acid, 1.2units/mL isocitric acid dehydrogenase and 1mM NADP. The human liver microsomal pool, HLM 1 (n = 22), HLM 2 (n = 50) and HLM 3 (n = 33) were purchased from BD Gentest (Woburn, MA); HLM 2 was kindly provided by Pfizer (Pharmacokinetics, Dynamics and Metabolism Department). The human intestinal microsomal pool (n = 10) was purchased from XenoTech (Kansas City, KS) and were prepared by elution method to ensure high enzyme activity, as reported previously (Galetin and Houston, 2006).

The final substrate concentration was 10-fold below the reported $K_m$ values in the literature for the drugs investigated. In the cases of indinavir and saquinavir, a substrate concentration of 0.1μM was used. The drug was added from methanol stock solution resulting in a final concentration of organic solvent in the incubation of 0.1%v/v. Clearance incubations were prepared as replicates of two in Eppendorf tubes at 37°C and 900rpm in an Eppendorf Thermomixer. The metabolic reaction was initialized by adding warm NADP solution to warm incubation mixture and samples were taken at 6 designated time points within 60 minutes. To monitor non-P450 dependent loss of drug over the incubation time additional

7

samples were prepared in the absence of NAPD. Metabolic reaction was terminated by addition of an equal volume of ice-cold acetonitrile containing the internal standard and samples were centrifuged at 1,000g for 20 minutes at 4°C in a Mistral 3001 centrifuge (MSE) and 150μL supernatant was removed from each Eppendorf vial and transferred to MVA glass vials (VWR International, Leicestershire, UK) prior to analysis on the LC-MS/MS system. Samples were embedded in the calibration curves upon LC-MS/MS analysis. $CL_{int}$ data were obtained for all drugs in the dataset, with the exception of alprazolam, quinidine and triazolam; for these CYP3A substrates data were taken from a previous in house study (Galetin and Houston, 2006).

**Microsomal Binding.** Nonspecific binding values of drugs to microsomal protein ($fu_{inc}$) were experimentally determined at different microsomal protein concentrations in HLM 1 using microdialysis method (Gertz et al., 2008b). In addition to reported experimental values in Gertz et al. (2008b), $fu_{inc}$ values for alfentanil, atorvastatin, cisapride, lovastatin, methadone, nisoldipine, rifabutin, sildenafil, trazodone and zolpidem were determined at 0.1, 0.5 and 1.0mg/mL microsomal protein concentrations over 8h. The $fu_{inc}$ values were fitted in Grafit 5.0.10 (Erithacus Software Limited) against protein concentrations to determine the binding constant ($K_a$). The drug specific $K_a$ values are summarized in the supplementary material on http://www.pharmacy.manchester.ac.uk/capkr/. In the case of cyclosporine, the extent of nonspecific binding was predicted (Hallifax and Houston, 2006).

The unbound intrinsic clearance values, $CLu_{int}$, were calculated using Eq. 4. Clearance values were corrected for the different organ abundances of CYP3A in liver and intestinal microsomes; 50 and 155pmolCYP3A/mg protein for the small intestine and the liver, respectively (Paine et al., 1997; Rostami-Hodjegan and Tucker, 2007).

$$CLu_{int} = \frac{V \cdot k}{protein_{microsomal}} \cdot \frac{1}{fu_{inc} \cdot Abundance_{CYP3A}} \qquad \text{Eq. 4}$$

$CLu_{int}$ (μL/min/pmolCYP3A); k, depletion rate constant (min$^{-1}$), V, initial incubation volume (mL); protein$_{microsomal}$, initial amount of protein (mg); Abundance$_{CYP3A}$ (pmolCYP3A/mg protein)

**Testosterone 6β-hydroxylation activity.** CYP3A enzyme activities of the HLM and HIM pools were determined at 250µM testosterone concentration (equivalent to $V_{max}$) monitoring 6β-hydroxytestosterone formation. Incubation conditions were the same as those used in the depletion assay; organic solvent content was 0.3%v/v methanol. Microsomal protein concentration for the HLM and HIM pools were 0.25 and 0.50mg/mL, respectively. On each occasion, three samples were taken after 5 minutes incubation. Aliquots of 100µL were removed into Eppendorf vials with 100µL ice cold acetonitrile containing 1µM progesterone as internal standard. Activity determination was performed on three separate occasions to account for inter-day variability. Mean and standard deviation for testosterone 6ß-hydroxylation activities were: 3.38 ±0.323, 4.48 ±0.218, 6.09 ±0.195 for HLM pool 1, 2 and 3, respectively, and 1.84 ±0.173nmol/min/mg for HIM.

**Prediction of i.v. and oral clearance.** Oral and intravenous clearance values, $fu_p$ values and blood to plasma ratios ($R_b$) were collated from the literature for all compounds investigated (Table 2). References for all considered clinical studies are available in the supplementary material (http://www.pharmacy.manchester.ac.uk/capkr/). When multiple clinical studies were available, mean clearance values and associated 95% credible intervals were calculated by meta-analyses using fixed or random effects models in Winbugs v.1.4.3 (available on http://www.mrc-bsu.cam.ac.uk/bugs/) assuming log-normal distribution of $CL_{i.v.}$ and $AUC_{oral}$. Criteria to exclude studies from analysis were: non-Caucasian populations, nonlinear dose-AUC response, AUC reported over an insufficiently long time-course, analytical method inappropriate to determine the concentration of the drug of interest adequately and studies performed in elderly or patient populations.

In the case of fixed effects model, $lnCL_{i.v.}$ and $lnAUC_{oral} \sim N(\mu, \omega^2)$; where $AUC_{oral}$ represents the dose-normalized AUC; $\mu$ represents the log-transformed mean $CL_{i.v.}$ or mean $AUC_{oral}$ and $\omega$ represents the variance ($SD^2/N$). The fixed effects model was used for drugs for which sparse data were available; this model made no distributional assumption on $\omega$. The mean and variance of the untransformed variables are $\exp(\mu+0.5\omega^2)$ and $\exp(2\mu+\omega^2)(\exp(\omega^2)-1)$, respectively. Otherwise random effects models were used: $lnCL_{i.v.}$ and $lnAUC_{oral} \sim N(\mu,$

9

$\omega^2$); gamma distribution of $\omega$, or: modified random effects model (for midazolam $CL_{i.v.}$ only):

$\ln CL_{i.v.}$ and $\ln AUC_{oral} \sim N(\mu, \omega^2)$; accounting for the distribution of the true SD of study i; $SD_i$

$\sim N(SD_{mean,i}, SD_{precision,i})$, where $\omega$ and the true precision followed gamma distributions.

$CL_{int,h}$ values after intravenous and oral drug administration were obtained using Eq. 5 and Eq. 6, respectively (Pang and Rowland, 1977).

$$CL_{int,h} = \frac{CL_h}{fu_b \cdot \left(1 - \dfrac{CL_h}{Q_h}\right)}$$ 

Eq. 5

$$CL_{int,h} = \frac{D}{AUC \cdot fu_b} \cdot F_G F_a$$ 

Eq. 6

where $CL_h$ and D/AUC represent the hepatic blood clearance obtained from mean plasma data (Table 2) after correcting for renal clearance (where applicable) and the blood to plasma distribution ratio ($R_b$); $fu_b$, fraction unbound in blood; $Q_h$, average hepatic blood flow of 20.7mL/min/Kg (Kato et al., 2003); D, the oral drug dose (mg/kg); AUC, the area under drug concentration-time curve (mg.min/mL) and $F_a$ the fraction absorbed.

Clearance data for cisapride, lovastatin, simvastatin and terfenadine were only available after oral drug administration. Oral clearance data for cyclosporine were available for two different oral formulations (Sandimmune® and Neoral®) and both were used in the assessment. $R_b$ data were not available for lovastatin, nisoldipine and trazodone. Given the very high structural similarity between simvastatin and lovastatin, the $R_b$ value used for lovastatin was 0.57. The $R_b$ values of nisoldipine and trazodone were assumed to be 1. The $CL_{int,h}$ estimate of trazodone was not sensitive to changes in $R_b$, whereas nisoldipine $CL_{int,h}$ displayed a high sensitivity to changes in $R_b$. Dose-AUC response data were assessed where available in order to avoid any bias in $CL_{int,h}$ estimates from oral data. Furthermore, indinavir was excluded from the oral dataset as the high dose at which it is administered (400 to 800mg) was shown to significantly reduce its systemic clearance (Yeh et al., 1999).

The unbound $CLu_{int}$ from all HLM pools investigated (µL/min/mg protein) were scaled using the mean microsomal recovery of 40mg protein/g liver (Barter et al., 2007) and a liver weight of 21.4g liver/kg to give a predicted $CL_{int,h}$ in ml/min/kg.

**Determination of *in vitro* permeability.** Drug permeability experiments in Caco-2 and MDCK-MDR1 cells were performed at Pfizer (Pharmacokinetics, Dynamics and Metabolism Department). The permeability experiments were performed during the cell passages 11 to 32 for the MDCK-MDR1 cells and 25 to 35 for the Caco-2 cells. To determine the passive permeability of drugs with efflux ratios greater than 2, the P-gp inhibitor CP-100356 (Wandel et al., 1999) was coincubated at a concentration of 10µM. MDCK-MDR1 cells (250µL, density $2.5 \times 10^5$ cells/mL in MDCK-MDR1 cell media) were added to the apical sides of Costar HTS 24 well transwell plates and MDCK-MDR1 cell media (1mL) was added to the basolateral sides. Plates were incubated for 4 days in a LEEC Research Incubator (37°C under 5% $CO_2$ in air) prior to cell permeability experiments. One day before experiment, the cell media in the apical and basolateral sides of the plate was replaced by fresh media. The MDCK-MDR1 cell media consisted of Alpha MEM (500mL), fetal bovine serum (50mL), penicillin-streptomycin liquid (5mL), MEM non essential amino acids (5mL) and L-glutamine (5mL). In contrast, the Caco-2 cells (250µL, density of $1.6 \times 10^5$ cells/mL) were plated in BD Falcon HTS 24 well transwell plates. Caco-2 cells were ready for use after 3 weeks incubation in a LEEC Research Incubator (37°C under 5% $CO_2$ in air). Media was replaced on alternate weekdays by Caco-2 cell media; 250µL and 1mL into the apical and basolateral side, respectively. The cell media for the Caco-2 cells consisted of MEM (500mL), fetal bovine serum (100mL), MEM non essential amino acids (6mL), sodium pyruvate solution (6mL) and L-glutamine solution (6mL).

The incubation buffer was prepared from HEPES (2.38g) solubilized in HBSS (500mL) and titrated to pH 7.4 with 1M sodium hydroxide solution. Experiments were performed under isotonic conditions at pH 7.4. Nadolol (2µM) or Lucifer yellow (100µM in HBSS pH 7.4) were used as integrity markers. Lucifer yellow mediated fluorescence was measured on a Victor[2] 1420 Multilabel Reader (Perkin Elmer Lifescience, Wallac). $P_{app}$ (A-B) values of nadolol or lucifer yellow were calculated using Eq. 7; $P_{app}$ values < 10nm/s were indication of an intact cell monolayer. 1µL of the drug stock solution (in DMSO) was added to 10mL of HBSS pH 7.4 buffer containing nadolol; resulting in a final substrate

11

concentration of 0.1µM (final concentration of DMSO 0.03%v/v). For each plate metoprolol
and talinolol were co-incubated as positive controls for passive permeability and active efflux,
respectively; both were incubated at a final substrate concentration of 2µM. The substrates
and the positive controls were incubated in three separate wells in both directions. The plates
were placed in a LEEC Research Incubator (37°C under 5% $CO_2$ in air) on a shaker at
150rpm for 2 or 2.5h for the Caco-2 and MDCK-MDR1 cell permeability experiment,
respectively. The setup and sampling was performed on a Tecan, Genesis RSP 150 Robot.
Samples and calibration curves were added to acetonitrile and centrifuged for 20 minutes at
3,000rpm prior to analysis on LC-MS/MS system.

**Sample Analysis.** Quantification of samples was performed in Analyst v.1.4.1
software (Applied Biosystems). Permeability values were calculated in both directions using
Eq. 7; drug recovery was between 75 and 130% except where noted in Table 3. Apparent
permeability, $P_{app}$ and efflux ratio, ER data defined as $P_{app}$ (B-A)/$P_{app}$ (A-B), for metoprolol
and talinolol were assessed with every plate. $P_{app}$ (A-B) for metoprolol > 200nm/s and an ER
value for talinolol of > 5 were used as an indicator for a functional cell monolayer.

$$P_{app} = \frac{V_R}{(A \cdot C_0)} \cdot \frac{dC}{dt} \qquad\qquad \text{Eq. 7}$$

$V_R$, volume of the receiver chamber; A, surface area of the cell monolayer (0.33cm$^2$); $C_0$, initial
substrate concentration (µM), dC/dt, change of concentration over time

Metoprolol $P_{app}$ data were available for 11 and 9 occasions for the assessment of inter-day
variability of $P_{app}$ in MDCK-MDR1 and Caco-2 cells, respectively. Permeability data of the
drugs investigated were normalized for the mean metoprolol permeability to account for inter-
day variability. The mean $P_{app}$ (A-B) value and SD for metoprolol in MDCK-MDR1 cells
were 341 ±92nm/s and in Caco-2 cells 281 ±42nm/s. No permeability data could be
determined for nisoldipine, terfenadine and atorvastatin and literature values were taken:
atorvastatin: 60nm/s in Caco-2 cells (Xiaochun et al., 2000; Hochman et al., 2004);
terfenadine: 106nm/s in MDCK-MDR1 cells (Polli et al., 2001; Doan et al., 2002);

nisoldipine: >200nm/s given its structural similarity to nifedipine and nitrendipine which both show high permeability (Polli et al., 2001).

**LC-MS/MS analysis and list of chemicals.** Detailed information on LC-MS/MS analysis and the list of chemicals are provided in the supplementary material (http://www.pharmacy.manchester.ac.uk/capkr/).

**Regression analysis between *in vitro* and *in vivo* permeability.** A correlation between *in vivo* $P_{eff}$ and *in vitro* $P_{app}$ (A-B) data in MDCK-MDR1 cells was investigated. The $P_{eff}$ data have been obtained in the upper jejunum for a range of compounds (Lennernas, 2007). The corresponding $P_{app}$ data for this additional set of drugs were provided by Pfizer (Pharmacokinetics, Dynamics and Metabolism Department) and were used as a training set for the regression analysis between $P_{app}$ and $P_{eff}$ (Fig. 1). The $P_{app}$ values for this training set (determined at 2μM under isotonic conditions, pH 7.4) ranged from 2.4 to 442nm/s for amoxicillin and antipyrine, respectively. The $P_{eff}$ values ranged from 0.04 to 8.7µm/s for hydrochlorothiazide and ketoprofen, respectively. Permeability data for the training dataset are available in the supplementary material (http://www.pharmacy.manchester.ac.uk/capkr/). Considering that the *in vivo* permeability of amoxicillin, amiloride, cephalexin, and cyclosporine might be facilitated by active transport, the regression analysis was performed either using all drugs (subset A: n = 24) or drugs which were characterized by passive permeability (subset B: n = 20). The regression analysis and the standard error associated with the regression coefficient were calculated in Grafit 5.0.10 (Erithacus Software Limited). The precision of $P_{eff}$ predictions based on the regression analysis using subset A and B was determined. The linear correlation between $P_{app}$ and $P_{eff}$ was weak ($R^2$=0.40) for both subsets A and B. The coefficients of determination between the $\log P_{app}$ and $\log P_{eff}$ were 0.61 and 0.70 if subsets A or B were used, respectively. Equations based on the regression analysis of the subset A and B are shown in Eq. 8 and Eq. 9, respectively.

$$\log P_{eff} = 0.712 \times \log P_{app} - 1.05 \qquad\qquad \text{Eq. 8}$$

$$\log P_{eff} = 0.829 \times \log P_{app} - 1.30 \qquad\qquad \text{Eq. 9}$$

The respective slopes of the regression analysis were associated with standard errors of 17 and 15% for subset A and B, respectively. The standard errors associated with the regression equations resulted on average in a 2.2-fold deviation of the $P_{eff}$ predictions from unity.

In addition to data from MDCK-MDR1 generated in the present study, correlation between $P_{eff}$ and $P_{app}$ in Caco-2 cells (pH 7.4) was already available for 24 drugs from previous studies (Sun et al., 2002), as shown in Eq. 10. Regression equations from both cell lines (Eq. 9 and Eq. 10 for MDCK-MDR1 and Caco-2, respectively) were used for the prediction of $P_{eff}$ and consequently $F_G$ for drugs in the current study; their prediction success and application in the $Q_{Gut}$ model was assessed.

$$\log P_{eff} = 0.4926 \times \log P_{app} - 0.1454 \qquad \text{Eq. 10}$$

**Prediction of $P_{eff}$ from physicochemical data.** In addition to *in vitro* data, the physicochemical parameters, hydrogen bond donors and polar surface area were collated for all drugs investigated on http://pubchem.ncbi.nlm.nih.gov/. Using the Eq. 11, $P_{eff}$ data were predicted from these physicochemical parameters, as described previously (Winiwarter et al., 1998). The application of $P_{eff}$ values using this approach for the prediction of $F_G$ was assessed in comparison to other permeability approaches described above.

$$\log P_{eff} = -2.546 - 0.011 PSA - 0.278 HBD \qquad \text{Eq. 11}$$

PSA, polar surface area; HBD, hydrogen bond donor

Bias and precision in estimating $CL_{int,h}$ and $F_G$ by were calculated as geometric fold error (gmfe), Eq. 12, and rooted mean squared error (rmse), Eq. 13 (Sheiner and Beal, 1981; Fahmi et al., 2008). The gmfe does not allow over- and under-predictions to cancel each other out and indicates therefore an absolute deviation from the line of unity.

$$gmfe = 10^{\frac{1}{n}\sum \left| \log \left( \frac{predicted}{observed} \right) \right|} \qquad \text{Eq. 12}$$

$$rmse = \sqrt{\frac{1}{n} \sum \left( predicted - observed \right)^2} \qquad \text{Eq. 13}$$

where gmfe represents the geometric fold error; rmse, rooted mean squared error (units of the parameter investigated) and n, number of observations.

## Results

*In vitro* **clearance.** *In vitro* clearance data were obtained in pooled human intestinal microsomes (n=10) and three liver microsomal pools (in total, n = 105 donors). The $CLu_{int}$ values covered four orders of magnitude and ranged from 1.10 to 3,840µL/min/mg protein for zolpidem and nisoldipine, respectively for the HIM pool. In the HLM pools, $CLu_{int}$ values span over a similar range, from 10.9 to 9,790µL/min/mg protein for zolpidem and saquinavir, respectively. The correlation between the HIM and the mean HLM clearance was strong ($R^2$=0.98). The $CLu_{int}$ values (expressed per mg of protein) determined in HIM represented between 32-47% of the average HLM $CLu_{int}$. However, tacrolimus and midazolam showed particularly high $CLu_{int}$ values in HIM representing 63% and 79% of the average HLM clearance, respectively.

A direct comparison of $CLu_{int}$ obtained in HLM and in HIM after the correction for the tissue specific abundance of CYP3A is shown in Table 1. Corrected $CLu_{int}$ values in the HIM pool ranged from 0.022 to 76.7µL/min/pmolCYP3A for zolpidem and nisoldipine, respectively and from 0.106 to 48.1µL/min/pmolCYP3A in the HLM pools for zolpidem and saquinavir, respectively. Fig. 2 illustrates comparison of the $CLu_{int}$ values of the drugs investigated normalized for the population CYP3A abundance in the intestine and liver. Good agreement between the estimates was observed with 50% of the clearance values within 1.5-fold and 14% outside 2-fold of the line of unity. The most pronounced discrepancy in the HLM and HIM clearance was observed for midazolam ($CLu_{int}$ in HIM represented 246% of mean $CLu_{int}$ in HLM) and zolpidem ($CLu_{int}$ in HIM represented 21% of mean $CLu_{int}$ in HLM). After correction for tissue specific CYP3A abundance, the $CLu_{int}$ determined in the HIM pool represented 100-144% of the $CLu_{int}$ in the HLM pools and were not statistically different at a significance level of 5% (Student t-test).

The $CLu_{int}$ data obtained from the three different liver pools were compared and found to be significantly different (p<0.05). The highest clearance values were determined in HLM 3 pool, whereas clearance in HLM pools 1 and 2 represented 56-75% of the $CLu_{int}$

determined in this pool. The microsomal activity towards 6β-hydroxytestosterone was determined in all microsomal pools and ranged from 1.84 to 6.09nmol/min/mg in the HIM and the HLM batch 3, respectively. The activity determination for each microsomal batch was associated with low inter-day variability (≤10%). The coefficient of variation between the activities of the different HLM batches was 29%, comparable to the 31% average inter-batch variability in clearance for the drugs investigated. Most of the $CLu_{int}$ variability between different microsomal pools could be attributed to the differences in 6β-hydroxytestosterone activity ($R^2$=0.99). In the cases of midazolam, nifedipine, nisoldipine and tacrolimus only 49 to 73% of the changes in clearance could be attributed to differences in testosterone 6β-hydroxylation activity.

**Prediction of hepatic intrinsic clearance from i.v. and oral data.** A large body of clinical clearance data after i.v. drug administration was collated for the drugs investigated, with up to 30 clinical studies investigating 469 individuals available in the case of midazolam (Table 2). The systemic plasma clearance of midazolam was estimated at 6.16mL/min/kg (5.64, 6.72, 95% credible interval) using meta-analysis of literature data which corresponded to an $CL_{int,h}$ of 440mL/min/kg (364, 533, 95% credible interval). The database consisted of 21 drugs, as no i.v. clearance data were available for cisapride, lovastatin, simvastatin and terfenadine, with a range of *in vivo* systemic plasma clearance, varying from 0.76 to 28.3mL/min/kg for the i.v. data of alprazolam and buspirone, respectively (Table 2). The $fu_p$ ranged from 0.3 to 36% for nisoldipine and indinavir, respectively and the $CL_h$ ranged from 4 to ~100% of $Q_h$ in the case of tacrolimus and buspirone, respectively. Overall, 11 of the investigated drugs showed $CL_h$ equal to or greater than 50% of $Q_h$. The highest blood clearance values were observed for buspirone, indinavir and saquinavir (all >80% of $Q_h$).

A moderate correlation existed between the observed and the predicted $logCL_{int,h}$ values when the well-stirred liver model was used ($R^2$>0.65); 43% and 76% of the predictions were within 2- and 5-fold of unity, respectively. The most significant $CL_{int,h}$ under-predictions (≤20% of observed) were noted for atorvastatin (2.5%), buspirone (7.6%), repaglinide (7.9%), felodipine (10%) and sildenafil (20%). The use of the average HLM clearance data and a

16

mean microsomal recovery value of 40mg/g resulted in a median under-prediction of 19%, a 3.1-fold bias (gmfe) and a precision (rmse) of 4,140 (Fig. 3A). The bias was notably decreased with increasing microsomal CYP3A4 activity of the different liver pools; however, the precision of $CL_{int,h}$ predictions was not affected by the use of different HLM pools.

A substantial number of clinical studies were available after oral administration; for most drugs investigated data from $\geq$3 clinical studies were used in the meta-analyses. Analogous to the i.v. situation, midazolam studies were the most abundant, as 14 separate studies with 262 individuals in total were considered in the analysis. The oral clearance of midazolam was estimated at 24.2mL/min/kg (20.5, 28.5, 95% credible interval) which corresponded to an $CL_{int,h}$ of 402mL/min/kg (340, 473, 95% credible interval). Clinical studies with an oral dose of midazolam exceeding 10mg were excluded from the analysis due to possible nonlinear response in midazolam AUC. The oral clearance values ranged from 0.99 to 3,440mL/min/kg for alprazolam and saquinavir, respectively (Table 2). The contribution of the small intestine to oral clearance was incorporated using the $F_G$ values listed in Table 5, as shown in Eq. 6. Consequently, $CL_{int,h}$ values ranged from 3.22 to 16,800mL/min/kg for alprazolam and terfenadine, respectively. After correction for the drug specific $F_G$ values, the $CL_{int,h}$ values estimated from oral data corresponded to 93% of the i.v. estimate on average. Particular differences between i.v. and oral estimates were apparent for indinavir (where oral $CL_{int,h}$ represented 7% of i.v. data) and sildenafil (18%). In the cases of indinavir this was attributed to enzyme saturation/inhibition at the high dose at which this drug is generally administered and the data were subsequently excluded from the analysis.

The predictability of oral clearance from *in vitro* data generated in the current study was investigated. Fig. 3B displays the comparison of the predicted to the observed $CL_{int,h}$ from oral data; 38 and 65% of the predictions were within 2- and 5-fold, respectively. The median prediction success was 93% of the observed values (inter-quartile range: 33-204%). Accounting for $F_G$ decreased the overall degree of under-predictions from oral data, however, considerable under-prediction persisted for atorvastatin (1.9% of observed) buspirone (4.7%), repaglinide (13.4%), felodipine (13.8%) and terfenadine (17.5%). Significant over-prediction

was apparent for rifabutin (6-fold), simvastatin and lovastatin (7- and 8-fold, respectively). An improvement in the $CL_{int,h}$ prediction success relative to the analysis performed without the $F_G$ was apparent in the decrease in bias by 25% and marked increase in precision (32,600 vs. 4,030 without and with $F_G$ incorporated, respectively). The resulting bias and precision of the $CL_{int,h}$ prediction from $F_G$ corrected oral clearance data were highly comparable to the predictions of $CL_{int,h}$ from i.v. data.

*In vitro* **permeability.** The $P_{app}$ and the ER data were determined across MDCK-MDR1 and Caco-2 cells for the drugs investigated (Table 3). The permeability values ranged from 6 to 398nm/s for cyclosporine and buspirone, respectively, in the MDCK-MDR1 cells and from 4 to 324nm/s for saquinavir and midazolam, respectively, in the Caco-2 cells. Six drugs represented P-gp substrates in both cell lines (ER>2), namely cyclosporine, indinavir, quinidine, rifabutin, saquinavir and tacrolimus. The ER in the MDCK-MDR1 cells increased in the following rank order: quinidine < tacrolimus < rifabutin < indinavir < cyclosporine < saquinavir; and ranged from 4.4 to 75. A similar rank order of increasing ER was evident in the Caco-2 cell system and was as follows: tacrolimus < rifabutin < quinidine < cyclosporine < indinavir < saquinavir with the ER ranging from 2.1 to 57 (Table 3). Co-incubation with CP-100356 inhibited drug efflux mediated by P-gp and the resulting permeability was taken to represent the passive permeability of the drugs in the respective cell line assuming no additional transport mechanisms. A relatively small proportion of drugs investigated displayed low permeability ($\leq$ 100nm/s): 18% and 31% in the MDCK-MDR1 and Caco-2 cell systems, respectively. The $P_{app}$ data in the MDCK-MDR1 cell system were subject to considerable inter-day variability (27% based on 11 observations); the variability in the Caco-2 cells was 15% (based on 9 observations). The $P_{app}$ values of the drugs investigated across both cell systems displayed a high linear correlation ($R^2$=0.79). In general, $P_{app}$ values in the Caco-2 cell system were lower than those generated in MDCK-MDR1 cells but the absolute differences were minor. The $P_{app}$ values determined in Caco-2 cells represented on average 66-89% (95% CI) of MDCK-MDR1 cell values. The relationship between $P_{app}$ determined across Caco-2 and MDCK-MDR1 cells was best described by the following equation.

$$P_{app\,Caco-2} = 0.746 \times P_{app\,MDCK-MDR1}$$  Eq. 14

**$Q_{Gut}$ calibration.** Midazolam represents a drug with high apparent permeability and therefore its $Q_{Gut}$ value is expected to approach $Q_{ent}$. Therefore, midazolam $Q_{Gut}$ provides the possibility to normalize the $Q_{Gut}$ values of other drugs estimated from *in vitro* data. The choice of midazolam as a calibrator was foremost based on the large body of available *in vivo* studies reporting simultaneous i.v. and oral midazolam pharmacokinetic data, as well as midazolam $CLu_{int}$ values determined in four different microsomal systems. The $Q_{Gut}$ value of midazolam was estimated from the weighted mean of the *in vivo* $F_G$ data and the *in vitro* clearance data determined in the present study (Table 1). The $Q_{Gut}$ value of midazolam was estimated as 16.6L/h. This value was associated with considerable uncertainty (coefficients of variation were 31% when accounting for the variability of *in vivo* $F_G$ estimates alone and 61% when combined variability of the *in vivo* $F_G$ estimate and the *in vitro* $CLu_{int}$ data was accounted for). This value approached the $Q_{ent}$ value of 18L/h used in this study, suggesting no permeability limitations and supporting the use of midazolam as a $Q_{Gut}$ calibrator.

**Predictions of intestinal availability.** Permeability and *in vitro* clearance data were used for $F_G$ predictions using the $Q_{Gut}$ model by eight different methods (Fig. 4). Firstly, $P_{app}$ data determined across Caco-2 and MDCK-MDR1 cell monolayers were used directly. In addition, $P_{eff}$ data were estimated from the regression analysis to $P_{app}$ values from either Caco-2 or MDCK-MDR1 and from physicochemical properties. In the latter approaches, $Q_{Gut}$ data were investigated before and after calibration with midazolam $Q_{Gut}$. The results of the prediction bias and accuracy of different approaches for the entire dataset and for the subset of drugs with *in vivo* $F_G<0.5$ are summarized in Table 4. The best $F_G$ prediction success was apparent from the direct input of $P_{app}$ data as shown by the lowest bias and interquartile range of all approaches investigated (Table 4, 1). The use of permeability data obtained in the different cell lines investigated in the current study resulted in minor differences in $F_G$ prediction success. In contrast, the input of the $P_{eff}$ data from the regression analysis to $P_{app}$ data resulted in a larger bias regardless of the cell line used (Fig. 4A, Table 4); however, this

under-prediction trend was corrected after adjustment for midazolam $Q_{Gut}$. The analysis has also indicated that the use of these empirical regression equations for drugs with $P_{app}<10nm/s$ is problematic, as highlighted by considerable scatter in this area (Fig. 2). The use of polar surface area and hydrogen bonding potential resulted in the most biased $F_G$ predictions and significantly under-prediction of $F_G$ (p<0.05). Adjustment for midazolam as calibrator of $Q_{Gut}$ had negligible impact on the $F_G$ predictions from physicochemical properties and the under-prediction trend remained (Fig. 4; Table 4, 4).

Fig. 4B illustrates the high degree of prediction accuracy for drugs with *in vivo* $F_G$ values >0.5. In contrast, a subset of 11 drugs with *in vivo* $F_G$ <0.5 is comparatively poorly predicted and the degree of imprecision is considerably increased in comparison to drugs with low to moderate intestinal extraction (Fig. 4C, Table 4). Consistent over the entire set, the direct input of $P_{app}$ data resulted in the lowest bias and interquartile range in comparison to each of the different approaches investigated. In the case of indinavir, significant under-prediction was observed regardless of permeability parameter input. The choice to perform permeability experiments under isotonic conditions might have biased the $P_{app}$ (A-B) values for certain drugs in the dataset, as the intestinal pH in the duodenum and jejunum is <7 (Fallingborg et al., 1989). Considering that a significant impact of permeability to $F_G$ predictions was only apparent at drug permeability <100nm/s, the chosen *in vitro* conditions might have biased subsequent $F_G$ predictions of indinavir and saquinavir ($P_{app}<10nm/s$) and, to a minor extent quinidine ($P_{app}<100nm/s$ in Caco-2 cells).

Fig. 5 and Table 5 illustrate the comparison between predicted and observed $F_G$ values based on $P_{app}$ data from both cell lines; each outlier is identified by a number. Over-prediction was apparent for rifabutin (1), atorvastatin (2), buspirone (3) and tacrolimus (4). The average predicted tacrolimus $F_G$ was associated with a high degree of variability (indicated by the large error bars) driven by the highly variable *in vitro* clearance of this drug. Under-prediction was observed for simvastatin (5), saquinavir (6), terfenadine (7), felodipine (8) and indinavir (9). The degree of under-prediction was dependent on the use of permeability input and was particularly high for indinavir (17 – 33% of observed), saquinavir

(5 – 12%) and terfenadine (16 – 29%). The $Q_{Gut}$ values, hybrid parameter reflecting both drug

permeability and mucosal blood-flow, ranged from 2.4 to 16.6L/h for saquinavir and

midazolam, respectively (Table 5).

## Discussion

This study has evaluated the use of various sources of metabolism and permeability data for predicting $F_G$ using the $Q_{Gut}$ model. A group of 25 structurally diverse CYP3A4 substrates was used for this investigation with corresponding $F_G$ values *in vivo* ranging from 0.07-0.94 for lovastatin and alprazolam, respectively.

**In vitro clearance data.** A high degree of comparability was observed between *in vitro* clearance from HIM and three HLM pools for the dataset investigated, as illustrated in Fig. 2. This suggests that *in vitro* clearance between hepatic and intestinal microsomes can be extrapolated if enzyme abundance data are available and the contribution of P450 enzyme to drug metabolism is known. The current findings support our previous work (Galetin and Houston, 2006) where a good agreement between normalized hepatic and intestinal clearances was observed for a limited number of substrates for a range of P450 enzymes. No significant difference in the hepatic and intestinal clearances once normalized for the tissue specific CYP3A abundance supports their inter-changeable usability, as illustrated here in the $Q_{Gut}$ model. $CL_{int}$ data were normalized using reported population enzyme abundance data based on a meta-analysis of 241 liver samples (Rowland-Yeo et al., 2004; Rostami-Hodjegan and Tucker, 2007). Abundance data for both CYP3A and CYP3A4 in the liver (155 and 111pmol/mg, respectively) are associated with large coefficients of variation (67-119%). In the current study, actual CYP3A4 abundance was available only for HLM pool 2 (Pfizer, 138pmol/mg) which was within the reported population limits. Furthermore, the reported population abundance data are based on liver microsomes of Caucasian origin and consequently the HLM pools with a high Caucasian donor percentage should be selected to allow appropriate scaling with population estimates. In contrast to the liver data, intestinal data are characterized to a lesser extent, as the CYP3A and CYP3A4 abundance data are available from 31 individual of mixed ethnicity (Paine et al., 2006).

This study found a very strong linear correlation between clearance values determined in different microsomal pools and their respective testosterone 6β-hydroxylation

activity. The differences observed in microsomal enzyme activity between the pools contributed considerably to the prediction success of clearance. Considering the aforementioned, pools with small donor sizes might not be representative of the true population mean. Additionally, different substrate binding sites associated with the CYP3A4 enzyme probably explain this discrepancy (Galetin et al., 2003), as well as differing contribution of CYP3A4/CYP3A5 to drug clearance (Galetin et al., 2004; Huang et al., 2004) in comparison to the marker substrate testosterone (e.g. tacrolimus, saquinavir). However, while prediction bias was affected by the choice of microsomal pools, it had only a marginal effect on the precision of clearance predictions. The current analysis included three known inhibitors of CYP3A, namely indinavir, saquinavir and verapamil (Eagling et al., 1997; Wang et al., 2004; Ernest et al., 2005). To avoid biased clearance estimates, incubations were performed at a substrate concentration below $K_i$ (for competitive inhibitors) or $K_I$ (time-dependent inhibitors) and over a short ($\leq$30 minutes) time period. No apparent inhibition was evident in the depletion plots; however, it cannot be ruled out that enzyme inhibition *in vitro* might have biased the extrapolation of *in vivo* clearance.

**Prediction of hepatic intrinsic clearance from i.v. and oral data.** A variable degree of $CL_{int,h}$ prediction success from microsomal data has been reported in the literature (Obach, 1999; Ito and Houston, 2005; Riley et al., 2005). The current study found a low degree of under-prediction for the CYP3A4 substrates investigated. The prediction success of $CL_{int,h}$ from oral data was considerably improved in the current study when drug specific $F_G$ values were incorporated; this was particularly evident for atorvastatin, buspirone, cyclosporine, felodipine and nisoldipine. The $CL_{int,h}$ estimate from oral data represented 98% (79%, 117%, 95%CI) of the $CL_{int,h}$ estimate from i.v. data (when indinavir data were excluded) and the regression between both datasets was very strong ($R^2$=0.96) ranging over 4 orders of magnitude. The incorporation of $F_G$ led to $CL_{int,h}$ over-predictions for rifabutin, simvastatin and lovastatin which might question the accuracy of the *in vivo* $F_G$ estimates for these drugs. Similarly, in the case of indinavir poor prediction success for oral clearance was observed. This drug is administered at high dose resulting in corresponding hepatic inlet concentration

23

of 4µM after oral administration; therefore, saturation/inhibition of systemic indinavir metabolism might occur given its low $K_m$ (Chiba et al., 1997; Koudriakova et al., 1998) and $K_i$ values <1µM (Eagling et al., 1997).

Permeability experiments were performed in MDCK-MDR1 and Caco-2 cells at low substrate concentration (0.1µM) and in the presence of a P-gp inhibitor for the drugs with apparent drug efflux mediated by P-gp (ER≥2). Permeability data were of considerable importance for the $F_G$ predictions of drugs with $P_{app}$ (A-B)<100nm/s; in contrast, if drug permeability exceeded this value, $F_G$ predictions were mainly driven by *in vitro* clearance as the $Q_{Gut}$ model was reduced to a perfusion rate limited model. As single concentrations below the anticipated luminal concentration were used in the permeability assessment, consequently an over-estimation of the contribution of P-gp might have occurred. A more comprehensive *in vitro* assessment of P-gp mediated transport (e.g., full kinetic profiles and differential pH to account for variability *in vivo*) for the P-gp substrates in the current study would be beneficial in order to fully understand the contribution of P-gp to intestinal first-pass.

**Predictions of intestinal first-pass metabolism.** The $Q_{Gut}$ model accounts for the fact that a drug with low permeability will have a longer exposure to the metabolizing enzymes in the enterocytes (Rostami-Hodjegan and Tucker, 2004; Yang et al., 2007). For drugs with *in vitro* permeability exceeding 100nm/s, the hybrid function $Q_{Gut}$ (as defined in Eq. 9) is reduced to $Q_{ent}$ resulting in simple perfusion rate limited processes. Considering this and the large availability of *in vivo* intestinal first-pass metabolism data, midazolam, a highly permeable CYP3A substrate, was explored as a $Q_{Gut}$ calibrator. However, as no *in vivo* measure of $Q_{Gut}$ or $CL_{int,g}$ are available, this value is based on the assumption that predicted $CL_{int,g}$ represents an adequate measure for midazolam *in vivo* intestinal clearance. The variability associated with $CL_{int,g}$ and $F_G$ values propagates into the estimation of $Q_{Gut}$ estimates, resulting in a considerable uncertainty associated with this parameter.

Applying the $Q_{Gut}$ model resulted in a high $F_G$ prediction success for drugs with low intestinal first-pass metabolism ($F_G$>0.5) with indinavir representing the only significant outlier (Fig. 4B). In contrast, the prediction success was considerably reduced for the subset

of drugs with $F_G$<0.5 (Fig. 4C). This trend was also observed for the prediction success of $F_H$ (data not shown) with comparable bias and imprecision (gmfe: 2.9 vs. 2.5 for $F_G$ and $F_H$, respectively). Generally, direct input of $P_{app}$ (A-B) data from Caco-2 or MDCK-MDR1 cells resulted in the highest $F_G$ prediction success and is therefore recommended. Both cell models were considered in the present analysis as they represent common tools in the pharmaceutical industry to determine permeability of new chemical entities. In contrast, the use of a regression equation based on physicochemical properties and $P_{eff}$ should be avoided, as it resulted in significant under-prediction of $F_G$ for the current dataset. This may partly be explained by a number of drugs with very high PSA (>100Å$^2$) (e.g., indinavir, saquinavir and tacrolimus), as the validity of the existing regression equation (Winiwarter et al., 1998) was not established for drugs with those properties. As *in vivo* $P_{eff}$ data were available for cyclosporine and verapamil (Lennernas, 2007), these data were used in the current $F_G$ predictions.

The $F_G$ over-estimations observed for buspirone and atorvastatin are consistent with the under-prediction of hepatic clearance (<8% of observed). Furthermore, for both drugs $CL_h$ approaches $Q_h$ which impedes an accurate estimation of *in vivo* $F_G$ bearing in mind that this parameter is indirectly assessed from i.v./oral data. Indeed, while i.v./oral data for atorvastatin suggested a $F_G$ value of 0.24, grapefruit juice interaction data suggested a less extensive intestinal contribution to atorvastatin first-pass metabolism; $F_{G,GFJ}$=0.56 (Gertz et al., 2008a). In the case of tacrolimus, $F_G$ predictions were highly variable between different microsomal pools used within this study, showing a general over-prediction trend. In addition to CYP3A, tacrolimus undergoes UGT-mediated metabolism and the under-estimation of intestinal clearance might also be attributed to conjugative metabolism (Strassburg et al., 2001). However, as currently no absolute UGT abundance data exist to allow incorporation of UGT metabolism into $F_G$ predictions, the impact of this contributing pathway could not be assessed.

Under-prediction of $F_G$ was observed for a number of drugs, including terfenadine, saquinavir and indinavir. Terfenadine displayed considerable nonspecific binding even at low protein concentration and erroneous $fu_{inc}$ determination might have subsequently affected the

*in vitro* estimate of its clearance. In order to minimize any issues associated with the nonspecific binding, low microsomal protein concentrations were used and $fu_{inc}$ values were experimentally determined for all the drugs using microdialysis (Gertz et al., 2008b), with the exception of cyclosporine for which this value was predicted (Hallifax and Houston, 2006). In addition, the use of substrate concentrations 10-fold below $K_m$ may over-estimate intestinal clearance given the high anticipated drug concentration in the enterocytes during the absorption phase. Potential saturation of CYP3A and P-glycoprotein *in vivo* (e.g., saquinavir*)* and the region of the intestine in which drug is absorbed also need to be considered when interpreting $F_G$ under-prediction observed. Some of the substrates for which $F_G$ is under-predicted represent either time-dependent or reversible inhibitors of CYP3A (i.e., indinavir and saquinavir) which may affect their *in vivo* estimates of $F_G$. Finally, one must not forget that the *in vivo* estimates of $F_G$ represent indirect assessments of the intestinal first-pass metabolism liable to several assumptions. In particular for drugs with low and variable bioavailability where $CL_h/Q_h$ approaches 1 (buspirone, felodipine, indinavir, lovastatin and saquinavir), delineation of the intestinal and hepatic contribution to first-pass metabolism is virtually impossible utilizing the i.v./oral approach.

In conclusion, this study has comprehensively investigated the suitability of the $Q_{Gut}$ model to predict $F_G$ for drugs with differential clearance and permeability characteristics. While drugs with low intestinal extraction were generally well predicted, the prediction success for drugs with high intestinal extraction ($F_G < 0.5$) was considerably less accurate and requires further refinement.

**Acknowledgements**

# References

Badhan R, Penny J, Galetin A and Houston JB (2009) Methodology for development of a physiological model incorporating CYP3A and P-glycoprotein for the prediction of intestinal drug absorption. *J Pharm Sci* **98:**2180-2197.

Barter ZE, Bayliss MK, Beaune PH, Boobis AR, Carlile DJ, Edwards RJ, Houston JB, Lake BG, Lipscomb JC, Pelkonen OR, Tucker GT and Rostami-Hodjegan A (2007) Scaling factors for the extrapolation of in vivo metabolic drug clearance from in vitro data: reaching a consensus on values of human microsomal protein and hepatocellularity per gram of liver. *Curr Drug Metab* **8:**33-45.

Chalasani N, Gorski JC, Patel NH, Hall SD and Galinsky RE (2002) Reply to Rostami-Hodjegan and Tucker 2002; Hepatology 35 (5): 1549-1550. *Hepatology* **35:**1550-1551.

Chiba M, Hensleigh M and Lin JH (1997) Hepatic and intestinal metabolism of indinavir, an HIV protease inhibitor, in rat and human microsomes: Major role of CYP3A. *Biochem Pharmacol* **53:**1187-1195.

Doan KMM, Humphreys JE, Webster LO, Wring SA, Shampine LJ, Serabjit-Singh CJ, Adkison KK and Polli JW (2002) Passive Permeability and P-Glycoprotein-Mediated Efflux Differentiate Central Nervous System (CNS) and Non-CNS Marketed Drugs. *J Pharmacol Exp Ther* **303:**1029-1037.

Eagling VA, Back DJ and Barry MG (1997) Differential inhibition of cytochrome P450 isoforms by the protease inhibitors, ritonavir, saquinavir and indinavir. *Br J Clin Pharmacol* **44:**190-194.

Ernest CS, 2nd, Hall SD and Jones DR (2005) Mechanism-based inactivation of CYP3A by HIV protease inhibitors. *J Pharmacol Exp Ther* **312:**583-591.

Fahmi OA, Maurer TS, Kish M, Cardenas E, Boldt S and Nettleton D (2008) A combined model for predicting CYP3A4 clinical net drug-drug interaction based on CYP3A4 inhibition, inactivation, and induction determined in vitro. *Drug Metab Dispos* **36:**1698-1708.

Fallingborg J, Christensen LA, Ingeman-Nielsen M, Jacobsen BA, Abildgaard K and Rasmussen HH (1989) pH-profile and regional transit times of the normal gut measured by a radiotelemetry device. *Aliment Pharmacol Ther* **3:**605-613.

Galetin A, Brown C, Hallifax D, Ito K and Houston JB (2004) Utility of recombinant enzyme kinetics in prediction of human clearance: impact of variability, CYP3A5, and CYP2C19 on CYP3A4 probe substrates. *Drug Metab Dispos* **32:**1411-1420.

Galetin A, Clarke SE and Houston JB (2003) Multisite kinetic analysis of interactions between prototypical CYP3A4 subgroup substrates: midazolam, testosterone, and nifedipine. *Drug Metab Dispos* **31:**1108-1116.

Galetin A, Gertz M and Houston JB (2008) Potential role of intestinal first-pass metabolism in the prediction of drug-drug interactions. *Expert Opin Drug Metab Toxicol* **4:**1-14.

Galetin A, Gertz M and Houston JB (2010) Contribution of intestinal cytochrome p450-mediated metabolism to drug-drug inhibition and induction interactions. *Drug Metab Pharmacokinet* **25:**28-47.

Galetin A and Houston JB (2006) Intestinal and Hepatic Metabolic Activity of Five Cytochrome P450 Enzymes: Impact on Prediction of First-Pass Metabolism. *J Pharmacol Exp Ther* **318:**1220-1229.

Gertz M, Davis JD, Harrison A, Houston JB and Galetin A (2008a) Grapefruit juice-drug interaction studies as a method to assess the extent of intestinal availability: utility and limitations. *Curr Drug Metab* **9:**785-795.

Gertz M, Kilford PJ, Houston JB and Galetin A (2008b) Drug lipophilicity and microsomal protein concentration as determinants in the prediction of the fraction unbound in microsomal incubations. *Drug Metab Dispos* **36:**535-542.

Granger DN, Richardson PD, Kvietys PR and Mortillaro NA (1980) Intestinal blood flow. *Gastroenterology* **78:**837-863.

Hall SD, Thummel KE, Watkins PB, Lown KS, Benet LZ, Paine MF, Mayo RR, Turgeon DK, Bailey DG, Fontana RJ and Wrighton SA (1999) Molecular and physical mechanisms of first-pass extraction. *Drug Metab Dispos* **27:**161-166.

Hallifax D and Houston JB (2006) Binding of Drugs to Hepatic Microsomes: Comment and Assessment of current prediction Methodology with Recommendation for Improvement. *Drug Metab Dispos* **34:**724-726.

Hochman JH, Pudvah N, Qiu J, Yamazaki M, Tang C, Lin JH and Prueksaritanont T (2004) Interactions of Human P-glycoprotein with Simvastatin, Simvastatin Acid, and Atorvastatin. *Pharm Res* **21:**1686.

Huang W, Lin YS, McConn DJ, 2nd, Calamia JC, Totah RA, Isoherranen N, Glodowski M and Thummel KE (2004) Evidence of significant contribution from CYP3A5 to hepatic drug metabolism. *Drug Metab Dispos* **32:**1434-1445.

Ito K and Houston JB (2005) Prediction of human drug clearance from in vitro and preclinical data using physiologically based and empirical approaches. *Pharm Res* **22:**103-112.

Ito K, Kusuhara H and Sugiyama Y (1999) Effects of intestinal CYP3A4 and P-glycoprotein on oral drug absorption--theoretical approach. *Pharm Res* **16:**225-231.

Jamei M, Turner D, Yang J, Neuhoff S, Polak S, Rostami-Hodjegan A and Tucker G (2009) Population-based mechanistic prediction of oral drug absorption. *Aaps J* **11:**225-237.

Kato M, Chiba K, Hisaka A, Ishigami M, Kayama M, Mizuno N, Nagata Y, Takakuwa S, Tsukamoto Y, Ueda K, Kusuhara H, Ito K and Sugiyama Y (2003) The intestinal first-pass metabolism of substrates of CYP3A4 and P-glycoprotein-quantitative analysis based on information from the literature. *Drug Metab Pharmacokinet* **18:**365-372.

Koudriakova T, Iatsimirskaia E, Utkin I, Gangl E, Vouros P, Storozhuk E, Orza D, Marinina J and Gerber N (1998) Metabolism of the Human Immunodeficiency Virus Protease Inhibitors Indinavir and Ritonavir by Human Intestinal Microsomes and Expressed Cytochrome P4503A4/3A5: Mechanism-Based Inactivation of Cytochrome P4503A by Ritonavir. *Drug Metab Dispos* **26:**552-561.

Lennernas H (2007) Intestinal permeability and its relevance for absorption and elimination. *Xenobiotica* **37:**1015-1051.

Lin JH, Chiba M and Baillie TA (1999) Is the role of the small intestine in first-pass metabolism overemphasized? *Pharmacol Rev* **51:**135-158.

Obach RS (1999) Prediction of Human Clearance of Twenty-Nine Drugs from Hepatic Microsomal Intrinsic Clearance Data: An Examination of In Vitro Half-Life Approach and Nonspecific Binding to Microsomes. *Drug Metab Dispos* **27:**1350-1359.

Paine MF, Hart HL, Ludington SS, Haining RL, Rettie AE and Zeldin DC (2006) The human intestinal cytochrome P450 "pie". *Drug Metab Dispos* **34:**880-886.

Paine MF, Khalighi M, Fisher JM, Shen DD, Kunze KL, Marsh CL, Perkins JD and Thummel KE (1997) Characterization of interintestinal and intraintestinal variations in human CYP3A-dependent metabolism. *J Pharmacol Exp Ther* **283:**1552-1562.

Pang KS and Rowland M (1977) Hepatic clearance of drugs. I. Theoretical considerations of a "well-stirred" model and a "parallel tube" model. Influence of hepatic blood flow, plasma and blood cell binding, and the hepatocellular enzymatic activity on hepatic drug clearance. *J Pharmacokinet Biopharm* **5:**625-653.

Polli JW, Wring SA, Humphreys JE, Huang L, Morgan JB, Webster LO and Serabjit-Singh CS (2001) Rational Use of in Vitro P-glycoprotein Assays in Drug Discovery. *J Pharmacol Exp Ther* **299:**620-628.

Riley RJ, McGinnity DF and Austin RP (2005) A unified model for predicting human hepatic, metabolic clearance from in vitro intrinsic clearance data in hepatocytes and microsomes. *Drug Metab Dispos* **33:**1304-1311.

Rostami-Hodjegan A and Tucker G (2004) `In silico' simulations to assess the `in vivo' consequences of `in vitro' metabolic drug-drug interactions. *Drug Discov Today* **1:**441.

Rostami-Hodjegan A and Tucker GT (2002) The Effects of Portal Shunts on Intestinal Cytochrome P450 3A Activity. *Hepatology* **35:**1549-1550.

Rostami-Hodjegan A and Tucker GT (2007) Simulation and prediction of in vivo drug metabolism in human populations from in vitro data. *Nat Rev Drug Discov* **6:**140.

Rowland-Yeo, Rostami-Hodjegan A and Tucker GT (2004) Abundance of cytochrome P450 in human liver: a meta-analysis. *Br J Clin Pharmacol* **57:**687-688.

Sheiner LB and Beal SL (1981) Some suggestions for measuring predictive performance. *J Pharmacokinet Biopharm* **9:**503-512.

Strassburg CP, Barut A, Obermayer-Straub P, Li Q, Nguyen N, Tukey RH and Manns MP (2001) Identification of cyclosporine A and tacrolimus glucuronidation in human liver and the gastrointestinal tract by a differentially expressed UDP-glucuronosyltransferase: UGT2B7. *J Hepatol* **34:**865-872.

Sun D, Lennernas H, Welage LS, Barnett JL, Landowski CP, Foster D, Fleisher D, Lee KD and Amidon GL (2002) Comparison of human duodenum and Caco-2 gene expression profiles for 12,000 gene sequences tags and correlation with permeability of 26 drugs. *Pharm Res* **19:**1400-1416.

Tam D, Sun H and Pang KS (2003) Influence of P-glycoprotein, transfer clearances, and drug binding on intestinal metabolism in Caco-2 cell monolayers or membrane preparations: a theoretical analysis. *Drug Metab Dispos* **31:**1214-1226.

Wandel C, Kim RB, Kajiji S, Guengerich P, Wilkinson GR and Wood AJ (1999) P-glycoprotein and cytochrome P-450 3A inhibition: dissociation of inhibitory potencies. *Cancer Res* **59:**3944-3948.

Wang YH, Jones DR and Hall SD (2004) Prediction of cytochrome P450 3A inhibition by verapamil enantiomers and their metabolites. *Drug Metab Dispos* **32:**259-266.

Winiwarter S, Bonham NM, Ax F, Hallberg A, Lennernas H and Karlen A (1998) Correlation of Human Jejunal Permeability (in Vivo) of Drugs with Experimentally and Theoretically Derived Parameters. A Multivariate Data Analysis Approach. *J. Med. Chem.* **41:**4939-4949.

Xiaochun W, Lloyd RW and Barbra HS (2000) Atorvastatin Transport in the Caco-2 Cell Model: Contributions of P-Glycoprotein and the Proton-Monocarboxylic Acid Co-Transporter. *Pharm Res* **V17:**209-215.

Yang J, Jamei M, Yeo KR, Tucker GT and Rostami-Hodjegan A (2007) Prediction of intestinal first-pass drug metabolism. *Curr Drug Metab* **8:**676-684.

Yeh KC, Stone JA, Carides AD, Rolan P, Woolf E and Ju WD (1999) Simultaneous investigation of indinavir nonlinear pharmacokinetics and bioavailability in healthy volunteers using stable isotope labeling technique: study design and model-independent data analysis. *J Pharm Sci* **88:**568-573.

**FOOTNOTES**

**Legends for Figures**

Fig. 1: Comparison of $P_{app}$ (A-B) obtained at isotonic pH of 7.4 in MDCK-MDR1 cells and human $P_{eff}$ available from the literature (Lennernas, 2007) for 20 passively permeable drugs; line of best fit is described by: $logP_{eff} = 0.829 \times logP_{app} - 1.30$ where the dashed lines indicate uncertainty in the line of best fit, as a consequence of standard error associated with the parameter estimates of slope (15%) and intercept (17%).

Fig. 2: Comparison of $CLu_{int}$ (µL/min/pmol CYP3A) from HLM (mean ±SD, n=3) and HIM for 22 drugs; dashed line indicates a bias of 1.55-fold deviation from unity

Fig. 3: Comparison of predicted and observed $CL_{int,h}$ values. Panel A represents the comparisons of observed and predicted $CL_{int,h}$ values from i.v. data obtained with the well-stirred model for 21 drugs. Panel B represents the comparison of observed and predicted $CL_{int,h}$ values from oral data after correction for *in vivo* $F_G$ (corresponding values listed in Table 5). Dashed lines represent the observed prediction bias of 3.1- and 2.9-fold deviation from unity for A and B, respectively and error bars indicate the SD from the *in vitro* clearance experiments. Outliers identified represent: 1, rifabutin; 2 tacrolimus; 3, zolpidem; 4, sildenafil; 5, repaglinide; 6, atorvastatin; 7, buspirone; 8, felodipine; 9, terfenadine; 10, lovastatin and 11, simvastatin.

Fig. 4: Prediction success of $F_G$ using eight different permeability approaches in the $Q_{Gut}$ model. The average $CLu_{int}$ data from HLM and HIM were used. A, represents the log (predicted $F_G$/observed $F_G$) of the complete dataset of 25 drugs; whereas, B and C represent the prediction success of drugs with *in vivo* $F_G$ values above (n=14) and below 0.5 (n=11), respectively. Zero indicates unity and negative and positive values under- and over-predictions, respectively; * shown in the graph represent significant under-predictions (p < 0.05).

33

Fig. 5: $F_G$ predictions obtained using *in vitro* clearance (Table 1) and $P_{app}$ (A-B) data obtained in either Caco-2 (✱) or MDCK-MDR1 cells (□). The dashed lines represent 1.5-fold deviation from unity and error bars represent the SD associated with the $F_G$ predictions using different HLM and HIM pools. Outliers identified represent: 1, rifabutin; 2 atorvastatin; 3, buspirone; 4, tacrolimus; 5, simvastatin; 6, saquinavir; 7, terfenadine; 8, felodipine and 9, indinavir.

## Table 1

*Comparison of CLu$_{int}$ corrected for CYP3A abundance in liver and intestine for one HIM and three HLM pools. Data obtained for 22[*] CYP3A4 substrate represent the individual clearance and the average clearance of all HIM and HLM batches together with the associated coefficient of variation (CV)*

| Substrate | CLu$_{int}$ (µL/min/pmol CYP3A) | | | | | |
|---|---|---|---|---|---|---|
| | HIM | HLM | | | Mean (all) | CV (%) |
| | | 1 | 2 | 3 | | |
| Alfentanil | 0.950 | 0.550 | 0.737 | 1.33 | 0.890 | 37 |
| Atorvastatin | 0.272 | 0.279 | 0.296 | 0.573 | 0.355 | 41 |
| Buspirone | 2.17 | 1.60 | 1.47 | 2.12 | 1.84 | 19 |
| Cisapride | 2.74 | 1.77 | 1.56 | 2.45 | 2.13 | 26 |
| Cyclosporine | 0.396 | 0.228 | 0.598 | 0.675 | 0.474 | 43 |
| Felodipine | 23.4 | 8.40 | 13.5 | 16.6 | 15.5 | 41 |
| Indinavir | 6.00 | 2.60 | 3.90 | 4.70 | 4.30 | 32 |
| Lovastatin | 48.8 | 18.8 | 31.6 | 42.2 | 35.4 | 37 |
| Methadone | 0.072 | 0.105 | 0.152 | 0.177 | 0.126 | 37 |
| Midazolam | 6.80 | 1.70 | 2.70 | 3.80 | 3.75 | 58 |
| Nifedipine | 2.20 | 1.90 | 1.70 | 2.20 | 2.00 | 14 |
| Nisoldipine | 76.7 | 27.0 | 54.0 | 54.5 | 53.1 | 38 |
| Repaglinide | 0.472 | 0.594 | 0.865 | 1.02 | 0.737 | 34 |
| Rifabutin | 0.516 | 0.319 | 0.577 | 0.642 | 0.514 | 27 |
| Saquinavir | 60.7 | 42.4 | 38.8 | 63.2 | 51.3 | 24 |
| Sildenafil | 1.12 | 0.87 | 1.05 | 1.23 | 1.07 | 14 |
| Simvastatin | 69.6 | 36.1 | 47.6 | 53.7 | 51.7 | 27 |
| Tacrolimus | 13.2 | 2.7 | 7.0 | 10.4 | 8.33 | 54 |
| Terfenadine | 33.0 | 19.2 | 20.2 | 27.2 | 24.9 | 26 |
| Trazodone | 0.236 | 0.323 | 0.414 | 0.505 | 0.37 | 31 |
| Verapamil | 2.36 | 1.30 | 2.22 | 2.87 | 2.19 | 30 |
| Zolpidem | 0.022 | 0.070 | 0.104 | 0.144 | 0.085 | 61 |

The clearance values determined in HLM 1 pool represented 75% (65, 84, 95% CI) of the clearance determined in HLM 2 pool and 56% (50, 62, 95% CI) of the clearance determined in HLM 3 pool; whereas HLM 2 pool represented 75% (65, 84, 95% CI) of HLM 3 pool. *Clearance values for triazolam, alprazolam and quinidine were taken from Galetin and Houston, 2006.

**Table 2**

*Mean i.v. and oral plasma clearance data, number of datasets, blood to plasma ratios, fraction unbound in plasma and the observed and predicted intrinsic*

*clearance values for 25 drugs investigated*

| Substrate | *In-vivo* parameters | | | | | | $CL_{int,h}$[1] | | |
|---|---|---|---|---|---|---|---|---|---|
| | $fu_p$ | $R_b$ | i.v. plasma clearance[1] | N | oral plasma clearance[1] | N | i.v. | Oral | predicted[11] |
| Alfentanil | 0.086 | 0.63 | 4.19 (3.93, 4.46) | 4 | 11.4 (10.7, 12.2) | 4 | 71.8 | 73.9 | 116 (55, 176) |
| Alprazolam[2] | 0.29 | 0.85 | 0.76 (0.71, 0.82) | 2 | 0.99 (0.90, 1.10) | 14 | 2.76 | 3.22 | 7.3 |
| Atorvastatin | 0.02 | 0.55 | 8.93 | 1 | 226 (211, 241) | 7 | 2,070 | 2,710 | 50.8 (26.0, 75.5) |
| Buspirone | 0.05 | 0.81 | 28.3 | 1 | 1,170 (797, 1670) | 14 | 3,020 | 4,920 | 229 (178, 281) |
| Cisapride | 0.02 | 1.0 | - | - | 7.85 (7.08, 8.69) | 4 | - | 216 | 256 (186, 325) |
| Cyclosporine | 0.068 | 1.36 | 3.99[6] (3.50, 4.59) | 7 | 12.3[6,7] (9.92, 14.9) | 8 | 110 | 97[9] | 66.4 (30.6, 102) |
| Cyclosporine | 0.068 | 1.36 | 3.99[6] (3.50, 4.59) | 7 | 25.4[6,8] (20.4, 31.0) | 7 | 110 | 201[9] | 66.4 (30.6, 102) |
| Felodipine | 0.004 | 0.70 | 11.9 (11.4, 12.4) | 4 | 110 (88, 137) | 11 | 17,020 | 12,300 | 1,700 (1,080, 2,330) |
| Indinavir | 0.36 | 0.84[3] | 18.4 | 1 | 14.2 (13.1, 15.3) | 6 | 440 | 30.4[10] | 498 (342, 653) |
| Lovastatin | 0.043 | 0.57[4] | - | - | 329 (293, 368) | 5 | - | 535 | 4,100 (2,340, 5,852) |
| Methadone | 0.21 | 0.75 | 1.66 (1.49, 1.85) | 5 | 2.13 (1.94, 2.34) | 6 | 7.48 | 7.03 | 19.1 (13.6, 24.7) |
| Midazolam | 0.031 | 0.55 | 6.16 (5.64, 6.72) | 30 | 24.2 (20.5, 28.5) | 14 | 440 | 402 | 367 (209, 525) |
| Nifedipine | 0.044 | 0.67 | 7.55 (7.00, 8.14) | 3 | 15.6 (12.0, 17.5) | 14 | 378 | 245 | 255 (212, 298) |
| Nisoldipine | 0.003 | 1.0[5] | 14.4 (13.2, 15.6) | 4 | 319 (280, 361) | 5 | 15,900 | 11,700 | 5,990 (3,630, 8,350) |
| Quinidine[2] | 0.26 | 0.87 | 3.86 (3.42, 4.35) | 2 | 5.64 (5.18, 6.13) | 3 | 11.6 | 15.0 | 7.4 |
| Repaglinide | 0.015 | 0.60 | 7.76 | 1 | 13.7 (12.8, 14.8) | 21 | 1,380 | 815 | 110 (77.3, 142) |
| Rifabutin | 0.29 | 0.60 | 3.46 | 1 | 16.2 (12.8, 20.5) | 8 | 16.6 | 11.5 | 68.1 (42.4, 93.7) |
| Saquinavir | 0.028 | 0.74 | 12.9 (10.3, 16.0) | 2 | 3,440 | 1 | 2,920 | 6,640[9] | 6,390 (4,410, 8,360) |
| Sildenafil | 0.04 | 0.64 | 8.97 | 1 | 9.42 (8.72, 10.2) | 4 | 694 | 127 | 139 (113, 166) |
| Simvastatin | 0.06 | 0.57[3] | - | - | 387 (317, 469) | 18 | - | 903 | 6,080 (4,730, 7420) |
| Tacrolimus | 0.13 | 35 | 0.64[6] (0.57, 0.73) | 4 | 4.93[6] (4.09, 5.83) | 8 | 179 | 186 | 892 (313, 1,470) |

36

| | | | | | | | | | |
|---|---|---|---|---|---|---|---|---|---|
| Terfenadine | 0.03 | 1.0 | - | - | 1,260 | 1 | - | 16,800 | 2,940 (2,290, 3,600) |
| Trazodone | 0.07 | 1.0[5] | 2.14 (1.94, 2.34) | 3 | 2.27 (2.18, 2.37) | 8 | 34.1 | 26.9 | 54.9 (41.2, 68.6) |
| Triazolam[2] | 0.10 | 0.62 | 2.94 (2.77, 3.13) | 7 | 6.36 (5.92, 6.83) | 9 | 38.2 | 47.2 | 43.7 |
| Verapamil | 0.093 | 0.89 | 11.7 (11.0, 12.5) | 6 | 43.3 (39.1, 47.8) | 6 | 347 | 303 | 283 (165, 401) |
| Zolpidem | 0.08 | 0.76 | 4.25 (3.96, 4.55) | 2 | 5.14 (4.33, 6.06) | 11 | 71.8 | 50.8 | 14.1 (8.54, 19.6) |

-, data not available or not applicable; values in parenthesis represent the 95% credible intervals for i.v. and oral plasma clearance for drugs where more than one clinical study were available and 95% confidence intervals for the predicted $CL_{int,h}$; [1] i.v. and oral clearance data represent systemic plasma clearances. Observed $CL_{int,h}$ values after i.v. and oral administration were calculated using Eqs. 5 and 6, respectively after correcting plasma clearances for renal excretion and blood to plasma ratio ($CL_h = (CL_p - CL_{renal})/R_b$); [2] *In vitro* clearance ($CLu_{int}$) data were supplemented from Galetin and Houston (2006) for alprazolam: 8.46 and 0.515 µL/min/mg in HLM and HIM, respectively; quinidine, 6.60 and 2.13 µL/min/mg in HLM and HIM, respectively and triazolam, 51.2 and 4.73 µL/min/mg in HLM and HIM, respectively; [3] provided by Pfizer, Global Research and Development; [4] assumed to be the same as for simvastatin; [5] assumed to be 1; [6] Blood clearance data; [7] Oral clearance of cyclosporine Neoral®; [8] Oral clearance of cyclosporine Sandimmune®; [9] fraction absorbed 0.9 and 0.3 for cyclosporine and saquinavir, respectively, otherwise complete absorption was assumed; [10] Evidence for saturation *in vivo* (Yeh et al., 1999); [11] $CL_{int,h}$ predictions based on the mean in vitro clearance data from 3 HLM pools; References for all clinical studies are available in the supplementary material (http://www.pharmacy.manchester.ac.uk/capkr/)

37

## Table 3

*Database of $P_{app}$ and efflux ratio data for the $F_G$ dataset obtained in MDCK-MDR1 and*

*Caco-2 cells*

| Substrate[1] | PSA | HBD | MDCK-MDR1 | | Caco-2 | |
|---|---|---|---|---|---|---|
| | | | $P_{app}$ A-B (nm/s) | ER | $P_{app}$ A-B (nm/s) | ER |
| Alfentanil | 85.5 | 0 | 376 | 0.7 | 293 | 1.1 |
| Alprazolam | 43.1 | 0 | 369 | 0.9 | 255 | 0.9 |
| Buspirone | 69.6 | 0 | 398 | 1.0 | 254 | 1.1 |
| Cisapride | 86.1 | 3 | 299 | 0.6 | 299 | 0.9 |
| Cyclosporine | 278.8 | 5 | 6 | 20 | 5 | 5.6 |
| Felodipine | 64.6 | 1 | 139 | 0.5 | 42 | 1.0 |
| Indinavir | 118 | 4 | 19 | 12 | 12 | 15 |
| Lovastatin | 72.8 | 1 | 261 | 1.1 | 145 | 0.8 |
| Methadone | 20.3 | 0 | 259 | 1.4 | 219 | 1.2 |
| Midazolam | 30.2 | 0 | 369 | 0.8 | 324 | 1.0 |
| Nifedipine | 107.8 | 1 | 389 | 1.0 | 235 | 1.0 |
| Nisoldipine | 108 | 1 | n/d | - | n/d | - |
| Quinidine | 45.6 | 1 | 176 | 4.4 | 85 | 3.8 |
| Repaglinide | 78.9 | 2 | 282 | 1.0 | 241 | 0.6 |
| Rifabutin | 206 | 5 | 52 | 6.0 | 95 | 3.3 |
| Saquinavir | 166.8 | 6 | 8 | 75 | 4 | 57 |
| Sildenafil | 113 | 1 | 262 | 2.0 | 256 | 1.8 |
| Simvastatin | 72.8 | 1 | 215 | 1.3 | 68 | 0.7 |
| Tacrolimus | 178.4 | 3 | 105 | 4.6 | 131 | 2.1 |
| Terfenadine | 43.7 | 2 | n/d | - | n/d | - |
| Trazodone | 42.3 | 0 | 295 | 1.1 | 242 | 0.9 |
| Triazolam | 43.1 | 0 | 350 | 0.9 | 280 | 0.6 |
| Verapamil | 64 | 0 | 318 | 1.0 | 138 | 1.8 |
| Zolpidem | 37.6 | 0 | 365 | 1.0 | 319 | 1.1 |

[1] $P_{app}$ (A-B) data was supplemented from the literature for in the cases of atorvastatin: 60nm/s in Caco-2 cells (Xiaochun et al., 2000; Hochman et al., 2004); terfenadine: 106nm/s in MDCK-MDR1 cells (Polli et al., 2001; Doan et al., 2002); nisoldipine: > 200nm/s given its structural similarity to nifedipine and nitrendipine both show high permeability (Polli et al., 2001)

**Table 4**

*Description of bias (gmfe) and percentage within 1.5-fold of unity for predictions of the $F_G$*

*for either total set of 25 drugs or for a subset of 11 drugs where in vivo $F_G<0.5$; different*

*permeability approaches were used as defined in the footnote*

| Total set of drugs (n=25) | 1 | 2 | 3 | 4 |
|---|---|---|---|---|
| < 1.5-fold, % | 64 (60) | 52 (60) | 56 (60) | 44 (44) |
| gmfe | 1.82 (1.74) | 2.29 (2.14) | 1.89 (1.89) | 3.93 (3.34) |
| **Drugs with *in vivo* $F_G<0.5$ (n=11)** | | | | |
| < 1.5-fold, % | 27 (18) | 18 (27) | 9 (18) | 18 (9) |
| gmfe | 2.89 (2.67) | 4.15 (3.65) | 2.82 (2.74) | 9.55 (7.35) |

1, $P_{app}$ (A-B) data from Caco-2 (data in parentheses: MDCK-MDR1); 2, $P_{eff}$ data from correlation to $P_{app}$ (A-B) from Caco-2 (data in parentheses: MDCK-MDR1); 3, $P_{eff}$ data from correlation to $P_{app}$ (A-B) from Caco-2 (data in parentheses: MDCK-MDR1) calibrated for midazolam $Q_{Gut}$; 4, $P_{eff}$ data from correlation to in silico data (data in parentheses: calibrated for midazolam $Q_{Gut}$)

**Table 5**

*Predictions of $F_G$ (±SD) and $Q_{Gut}$ using the $Q_{Gut}$ model from in vitro clearance and*

*permeability data for 25 drugs*

| Substrate | $F_G$ | | $Q_{Gut}$ (L/h) |
|---|---|---|---|
| | predicted[1] | observed | estimated |
| Alfentanil | 0.82 ±0.06 | 0.60 | 16.6 |
| Alprazolam | 0.99 ±0.01 | 0.94 | 16.4 |
| Atorvastatin | 0.90 ±0.04 | 0.24 | 12.7 |
| Buspirone | 0.68 ±0.04 | 0.21 | 16.4 |
| Cisapride | 0.65 ±0.06 | 0.55 | 16.6 |
| Cyclosporine | 0.82 ±0.07[2] | 0.44 | 8.6[2] |
| Felodipine | 0.20 ±0.07 | 0.45 | 14.5 |
| Indinavir | 0.25 ±0.07 | 0.93 | 5.7[4] |
| Lovastatin | 0.10 ±0.04 | 0.07 | 15.4 |
| Methadone | 0.97 ±0.01 | 0.78 | 16.2 |
| Midazolam | 0.54 ±0.14 | 0.51 | 16.6 |
| Nifedipine | 0.66 ±0.03 | 0.74 | 16.3 |
| Nisoldipine | 0.08 ±0.03 | 0.11 | 16.3 |
| Quinidine | 0.99 ±0.001 | 0.90 | 13.9[4] |
| Repaglinide | 0.84 ±0.05 | 0.89 | 16.3 |
| Rifabutin | 0.87 ±0.03 | 0.21 | 14.3[4] |
| Saquinavir | 0.01 ±0.003 | 0.18[3] | 2.4[4] |
| Sildenafil | 0.78 ±0.02 | 0.54 | 16.4 |
| Simvastatin | 0.06 ±0.02 | 0.14 | 13.2 |
| Tacrolimus | 0.34 ±0.16 | 0.14 | 15.1 |
| Terfenadine | 0.11 ±0.02 | 0.40 | 11.9 |
| Trazodone | 0.91 ±0.03 | 0.83 | 16.3 |
| Triazolam | 0.95 ±0.04 | 0.75 | 16.5 |
| Verapamil | 0.67 ±0.07[2] | 0.65 | 15.2[2] |
| Zolpidem | 0.98 ±0.01 | 0.79 | 16.6 |

[1] $F_G$ predictions based on $Q_{Gut}$ model (Eq. 2) using Caco-2 $P_{app}$ (A-B) data; [2] estimates based on available human $P_{eff}$ data: cyclosporine 1.65 ±0.53μm/s and verapamil 6.8 ±2.9μm/s (Lennernas, 2007); [3] $F_G$ data was determined from saquinavir Invirase®, no data were available for saquinavir Fortovase®; [4] indinavir, quinidine, rifabutin and saquinavir $Q_{Gut}$ values were 13.8, 16.4, 15.9, 13.5L/h, respectively, if no additional contribution of P-gp was assumed (passive permeability only)
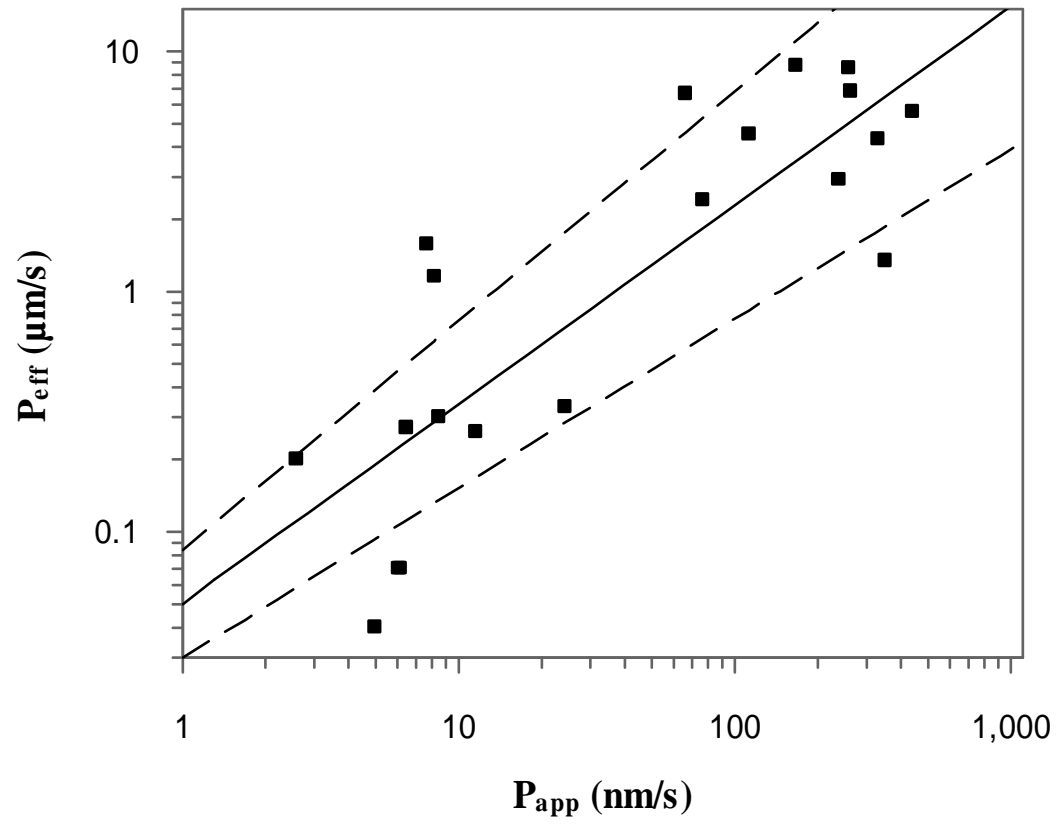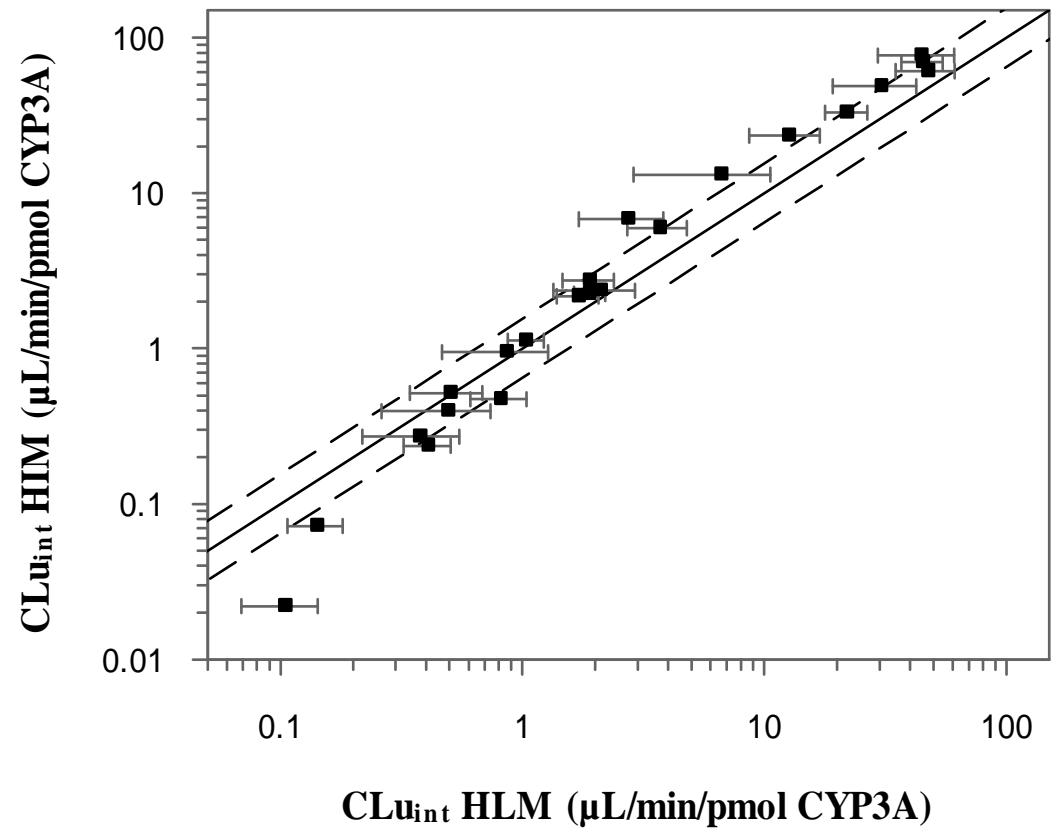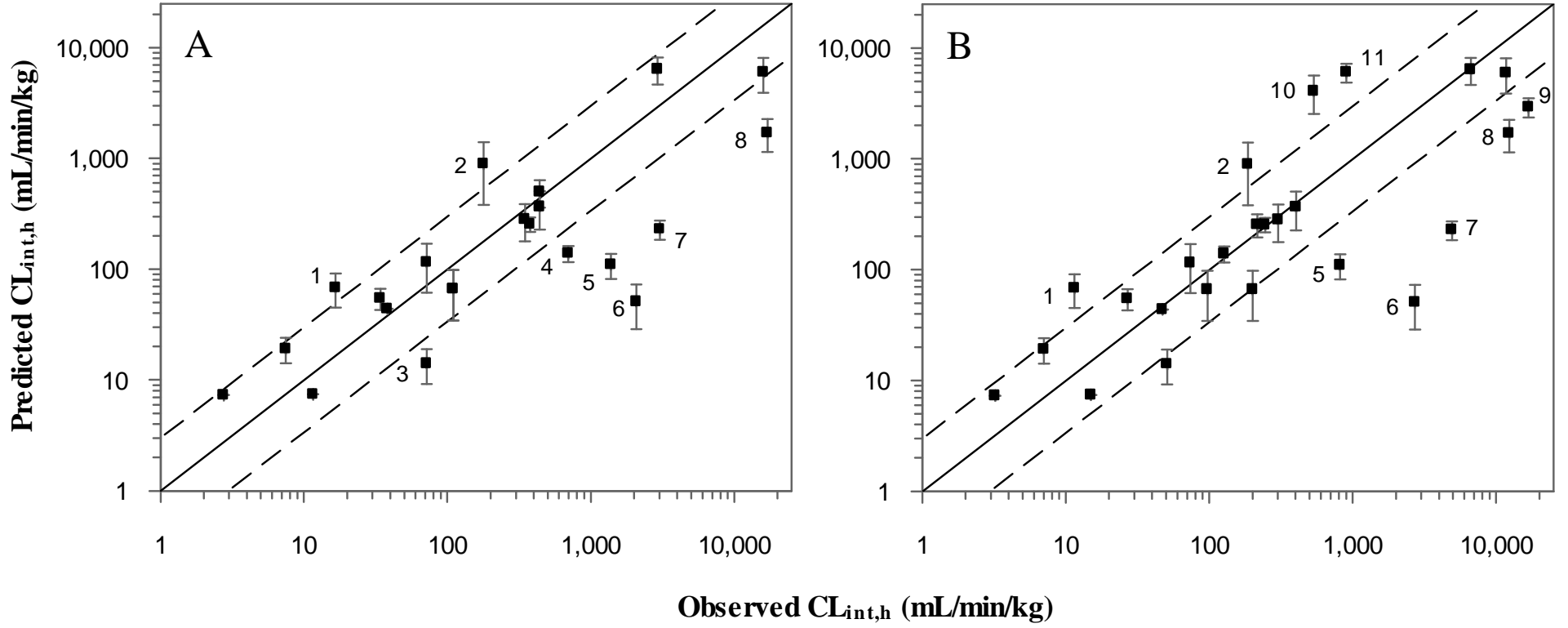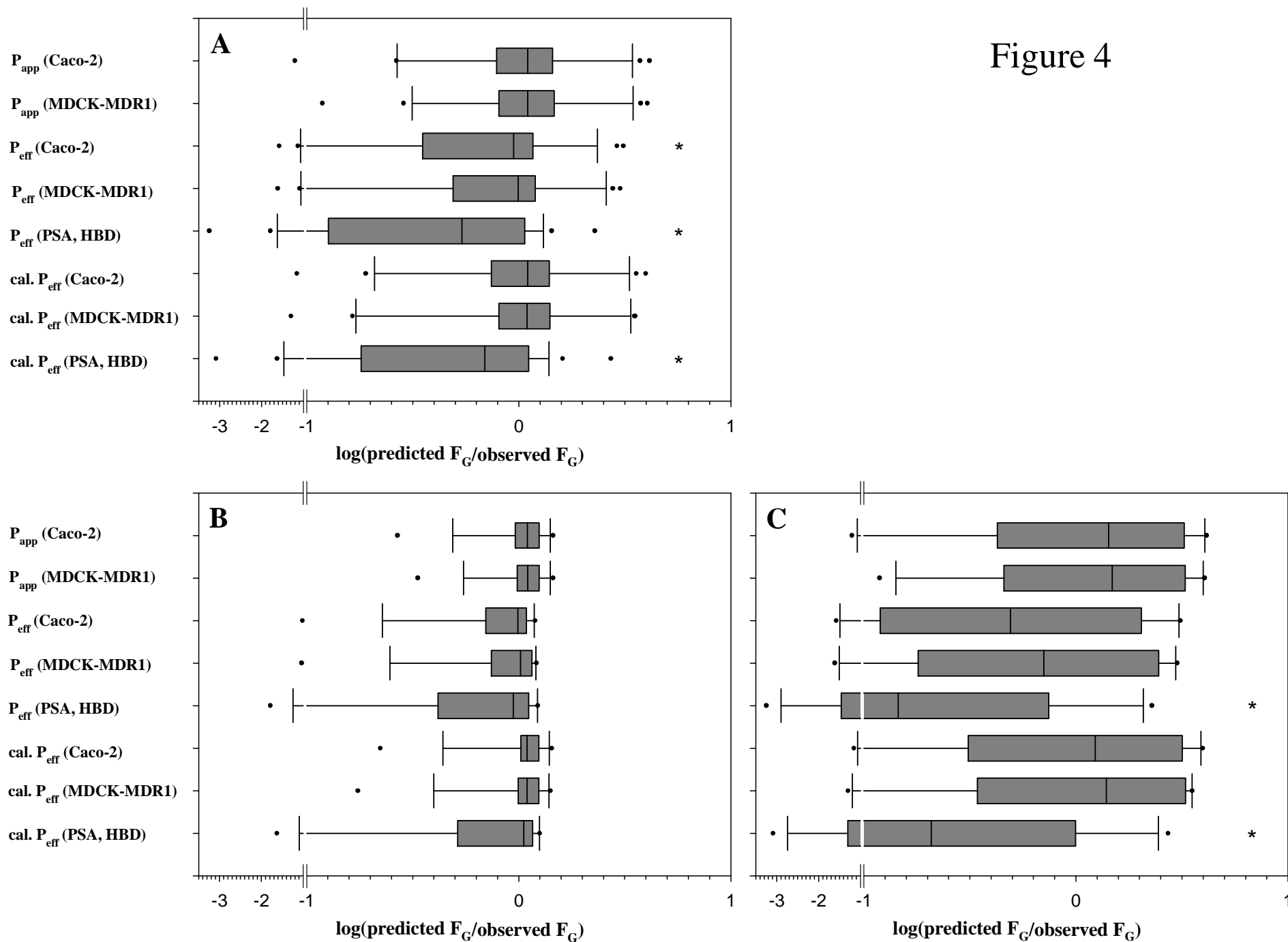
Figure 1

Figure 2

Figure 3

Figure 4

Figure 5